AIP Journal of Applied Physics

Atomic-layer deposited thulium oxide as a passivation layer on germanium

I. Z. Mitrovic, S. Hall, M. Althobaiti, D. Hesp, V. R. Dhanak, A. Santoni, A. D. Weerakkody, N. Sedghi, P. R. Chalker, C. Henkel, E. Dentoni Litta, P.-E. Hellström, M. Östling, H. Tan, and S. Schamm-Chardon

Citation: Journal of Applied Physics **117**, 214104 (2015); doi: 10.1063/1.4922121
View online: http://dx.doi.org/10.1063/1.4922121
View Table of Contents: http://scitation.aip.org/content/aip/journal/jap/117/21?ver=pdfcov
Published by the AIP Publishing

Articles you may be interested in
Epitaxy of polar semiconductor Co3O4 (110): Growth, structure, and characterization
J. Appl. Phys. **115**, 243708 (2014); 10.1063/1.4885048

X-ray photoelectron spectroscopy analysis and band offset determination of CeO2 deposited on epitaxial (100), (110), and (111)Ge
J. Vac. Sci. Technol. B **32**, 011217 (2014); 10.1116/1.4862160

Energy band alignment of atomic layer deposited HfO2 on epitaxial (110)Ge grown by molecular beam epitaxy
Appl. Phys. Lett. **102**, 093109 (2013); 10.1063/1.4794838

High quality Ge thin film grown by ultrahigh vacuum chemical vapor deposition on GaAs substrate
Appl. Phys. Lett. **98**, 161905 (2011); 10.1063/1.3580605

Impact of titanium addition on film characteristics of Hf O 2 gate dielectrics deposited by atomic layer deposition
J. Appl. Phys. **98**, 054104 (2005); 10.1063/1.2030407

Frustrated by old technology?
Is your AFM dead and can't be repaired?
RIP
My Old AFM 1994-2015
Sick of bad customer support?
It is time to upgrade your AFM
Minimum $20,000 trade-in discount for purchases before August 31st
Asylum Research is today's technology leader in AFM
dropmyoldAFM@oxinst.com
OXFORD INSTRUMENTS
The Business of Science®

[This article is copyrighted as indicated in the article. Reuse of AIP content is subject to the terms at: http://scitation.aip.org/termsconditions. Downloaded to] IP: 138.253.76.166 On: Wed, 03 Jun 2015 15:54:11

JOURNAL OF APPLIED PHYSICS 117, 214104 (2015)

Atomic-layer deposited thulium oxide as a passivation layer on germanium

I. Z. Mitrovic,[1,a)] S. Hall,[1] M. Althobaiti,[2] D. Hesp,[2] V. R. Dhanak,[2] A. Santoni,[3] A. D. Weerakkody,[1] N. Sedghi,[1] P. R. Chalker,[4] C. Henkel,[5,b)] E. Dentoni Litta,[5] P.-E. Hellström,[5] M. Östling,[5] H. Tan,[6] and S. Schamm-Chardon[6]

[1]*Department of Electrical Engineering and Electronics, University of Liverpool, Brownlow Hill, Liverpool L69 3GJ, United Kingdom*
[2]*Department of Physics and Stephenson Institute for Renewable Energy, University of Liverpool, Liverpool L69 7ZF, United Kingdom*
[3]*ENEA, Frascati Research Centre, via E. Fermi 45, 00044 Frascati, Italy*
[4]*Department of Engineering, University of Liverpool, Brownlow Hill, Liverpool L69 3GH, United Kingdom*
[5]*School of ICT, KTH Royal Institute of Technology, Isafjordsgatan 22, 164 40 Kista, Sweden*
[6]*CEMES-CNRS and Université de Toulouse, nMat group, BP 94347, 31055 Toulouse Cedex 4, France*

(Received 10 December 2014; accepted 23 May 2015; published online 3 June 2015)

A comprehensive study of atomic-layer deposited thulium oxide (Tm_2O_3) on germanium has been conducted using x-ray photoelectron spectroscopy (XPS), vacuum ultra-violet variable angle spectroscopic ellipsometry, high-resolution transmission electron microscopy (HRTEM), and electron energy-loss spectroscopy. The valence band offset is found to be 3.05 ± 0.2 eV for Tm_2O_3/p-Ge from the Tm 4d centroid and Ge $3p_{3/2}$ charge-corrected XPS core-level spectra taken at different sputtering times of a single bulk thulium oxide sample. A negligible downward band bending of ~0.12 eV is observed during progressive differential charging of Tm 4d peaks. The optical band gap is estimated from the absorption edge and found to be 5.77 eV with an apparent Urbach tail signifying band gap tailing at ~5.3 eV. The latter has been correlated to HRTEM and electron diffraction results corroborating the polycrystalline nature of the Tm_2O_3 films. The Tm_2O_3/Ge interface is found to be rather atomically abrupt with sub-nanometer thickness. In addition, the band line-up of reference GeO_2/n-Ge stacks obtained by thermal oxidation has been discussed and derived. The observed low reactivity of thulium oxide on germanium as well as the high effective barriers for holes (~3 eV) and electrons (~2 eV) identify Tm_2O_3 as a strong contender for interfacial layer engineering in future generations of scaled high-κ gate stacks on Ge. *© 2015 AIP Publishing LLC.*
[http://dx.doi.org/10.1063/1.4922121]

I. INTRODUCTION

Interface engineering plays a pivotal role in new high-κ/metal gate technology advancement.[1] Germanium has recently gained much interest as a high carrier mobility channel substitute to silicon in complementary metal oxide semiconductor (CMOS) devices together with the use of high-κ dielectric materials, such as HfO_2.[2,3] In contrast to superior interface properties of SiO_2/Si, Ge oxides are well-known to be thermally and chemically unstable.[4] Therefore, passivation of the Ge surface is a critical step for fabricating high performance Ge-based field effect transistors (FETs). The native oxide GeO_2 has attracted renewed research interest[5] as a potential passivation layer owing to its excellent interface control on Ge. However, for aggressive oxide scaling with equivalent oxide thickness (EOT) well below 1 nm, the combination of higher-κ rare-earth (RE) oxide and ultra-thin GeO_2 is required.[6] The thermodynamically robust interfacial layer (IL) engineering on Ge using RE Y_2O_3-doped GeO_2 has been shown recently to deliver 0.47 nm EOT on Ge, with superior interface properties and mobilities in Ge nMOSFETs.[6] Another approach to achieving sub-nm EOT Ge gate stacks is utilizing Al_2O_3 barrier IL properties.[2,3,7]

Rare-earth thulium oxide (Tm_2O_3) has been considered as the main high-k dielectric[8] and as a capping layer for La_2O_3-based gate stacks,[9] but only on Si. A low reactivity of Tm_2O_3 with the Si substrate has been observed.[10] There have been theoretical prediction and some recent estimations of the band gap (~5 eV,[11] ~6.5 eV,[12] and 5.76 eV,[13] respectively) on Tm_2O_3/Si structures. Atomic-layer deposition (ALD) has become one of the preferred methods for thin film deposition in several fields due to the excellent thickness control, uniformity, and conformality. A novel process for atomic-layer deposition of thulium oxide has been recently developed.[14] A TmSiO IL layer with EOT of ~0.25 nm has been achieved, which indicates a strong potential for its integration in sub-10 nm technology nodes.[15] Conversely, there have been no reports on Tm_2O_3 as a passivation layer on Ge, apart from our earlier work.[16]

A reliable measurement method to determine the band offsets is essential for modelling the carrier transport properties. The offsets reported at the GeO_2/Ge interface show large scattering in the range of about 1 eV for data obtained by x-ray photoelectron spectroscopy (XPS) and internal photoemission (IPE) (see Ref. 17 and references therein). Detailed mechanism responsible for such discrepancy is not clear. There are assumptions made that this is due to different GeO_2 growth methods.[5,18–23] Furthermore, it has come recently to focus that the XPS requires careful attention to

[a)]Author to whom correspondence should be addressed. Electronic mail: ivona@liverpool.ac.uk.
[b)]Current address: X-FAB Semiconductor Foundries AG, Erfurt, Germany.

 © 2015 AIP Publishing LLC

[This article is copyrighted as indicated in the article. Reuse of AIP content is subject to the terms at: http://scitation.aip.org/termsconditions. Downloaded to] IP: 138.253.76.166 On: Wed, 03 Jun 2015 15:54:11

charging effects as a result of electron emission from the insulator;[24–26] while the IPE data demand careful interpretation.[27] A clear understanding of the physical phenomena behind the charge accumulation and neutralization in dielectric/semiconductor heterojunction during XPS measurements seems still to be elusive.[25] A recent XPS study on HfO_2/Ge heterostructures[28] suggests that the role of germanium is not negligible in the neutralization mechanisms beyond the differential charging effect. Charging can occur in an XPS experiment when the holes that are created by the ejection of photoelectrons accumulate in a sample. This build-up of charge results in an increase in the binding energy (BE) of spectral features. Bersch *et al.*[26] have shown that not correcting for charging results in overestimation of valence band offset (VBO) by ~0.5 eV on average. It is common practice for the VBO to be determined from XPS measurements by Kraut's method using the valence band (VB) and core-level (CL) photoemission from bulk-like samples of the two constituent materials and a thin interfacial sample forming the interface of interest.[29] The overlayer of this heterojunction sample must be sufficiently thin (usually <5 nm) to allow XPS core-levels from the underlying material to be probed due to the finite escape depth of the photoelectrons. The binding energy values are referenced to the valence band maximum (VBM) of each sample, determined by extrapolating a linear fit of the leading edge of the VB photoemission to the baseline in order to account for broadening of the photoemission spectra.[30] Then, the VBO for oxide/semiconductor substrate sample can be determined as

$$\mathrm{VBO} = \delta_{\mathrm{SUB}} + \delta_{\mathrm{INT}} - \delta_{\mathrm{OXIDE}}, \tag{1}$$

where δ_{SUB} and δ_{OXIDE} are the energy differences between chosen reference core-levels in substrate and bulk oxide samples and their respective VBMs, while δ_{INT} refers to the BE difference for the former two core-levels for the interfacial sample.

This paper conveys three important findings: (i) the valence band offset for Tm_2O_3/Ge of 3.05 ± 0.2 eV, determined by Kraut's method[29] using a single sample consequently sputtered with core-level spectra taken at different sputtering times, shows consistency within experimental error with the offset result obtained using three distinctive samples (bulk, interfacial, and substrate);[16] (ii) the VBO for thermal GeO_2/Ge is in agreement with the most recent report from Toriumi's group[17] substantiating a conduction band offset (CBO) higher than 1 eV and the appropriateness of GeO_2 use in passivation of Ge; (iii) Tm_2O_3 shows even lower reactivity on Ge than on Si, with rather atomically sharp interface indicating possible barrier properties.

II. EXPERIMENTAL

The 10 nm (nominal) thick Tm_2O_3 samples were prepared by ALD on 35 nm p-Ge epitaxial layer/Si(100) and on Si(100). The reference samples of GeO_2 (5 and 10 nm nominal thicknesses) were grown on 35 nm n-Ge epi/Si(100) by thermal oxidation at 525 °C under 1 atm O_2. Prior to the gate oxide deposition, epi Ge/Si(100) samples were cleaned in a HF 0.5%/Isopropanol 1% /H_2O mixture to remove (minimize) the native Ge oxide layer. The Tm_2O_3 layers were deposited using Tris(cyclopentadienyl)thulium, heated to 140 °C, and water vapor as precursor gases.[14] An ultra-high vacuum (UHV) system operating at 4×10^{-8} Pa base pressure and equipped with a VG Al Kα monochromatized x-ray source and a CLAM2 hemispherical analyzer was used for XPS data acquisition at normal emission. The electron analyzer was set at constant 20 eV pass energy mode and calibrated.[31] The total energy resolution is found to be <0.7 eV from the fitting of the Fermi edge of a clean Au sample. The binding energy is referred to the position of the Fermi level measured on a clean Ta strip in good electrical contact with the sample. In order to reach the Tm_2O_3/Ge interface, the samples were mildly sputtered with 0.5 keV Ar^+ ion energy (0.25 nm/min). The main XPS core-levels and VB edge in the bulk Tm_2O_3 have been monitored as a function of sputtering time in order to reveal possible sputtering-induced effects. No change in the VB edge positions and in the Tm 4d and O 1s CL lineshapes, relative intensities, and BE positions could be detected by XPS after sputtering cycles, indicating that Ar^+ bombardment did not induce preferential sputtering and any observable surface modifications. The XPS spectra for GeO_2/n-Ge samples were recorded on a separate UHV system consisting of an Al Kα x-ray ($h\nu = 1486.6$ eV) source and a PSP Vacuum Technology electron energy analyzer. This spectrometer was calibrated so the Ag $3d_{5/2}$ photoelectron line had a BE of 368.35 eV, a full width at half maximum (FWHM) of 0.8 eV being the spectral resolution for this study, and a 10 eV pass energy. Charge compensation was achieved using a VG Scienta FG300 low energy electron flood gun with the gun settings adjusted for optimal spectral resolution. The electron BEs were then corrected by setting the C 1s peak in the spectra (due to stray carbon impurities) at 284.6 eV for all samples.[32] The probe area during the XPS measurements was 1 mm^2. The error bar (±0.2 eV) we defined in this paper is due to VBM determination through the linear interpolation method.[30] The core-level binding energy determination by fitting a Voigt curve to a measured peak introduces typically much smaller (±0.05 eV) error. A Shirley-type background[33] is used during the fitting of all spectra. The vacuum ultra-violet variable angle spectroscopic ellipsometry (VUV-VASE) measurements were performed using a spectral range from 0.5 to 8 eV, and the angles of incidence of 55°–75°, by 10° as a step, to maximize the accuracy. The atomic structure and elemental analysis were investigated with high-resolution transmission electron microscopy (HRTEM) and electron energy-loss spectroscopy (EELS) performed on a field emission image-corrected FEI Tecnai™ F20 microscope operating at 200 kV. For local EELS studies, the microscope was also equipped with a scanning stage (STEM), allowing a focused one nanometer-sized probe to be scanned over the sample area of interest (in our case, a line crossing the Tm_2O_3/Ge interface), and an imaging filter (Gatan GIF TRIDIEM) used as a spectrometer.

III. RESULTS AND DISCUSSION

A. Estimation of VBO for Tm_2O_3/Ge gate stack

The VBO determination of the Tm_2O_3/Ge system is addressed first. Fig. 1 shows high-resolution Tm 4d, valence

[This article is copyrighted as indicated in the article. Reuse of AIP content is subject to the terms at: http://scitation.aip.org/termsconditions. Downloaded to] IP: 138.253.76.166 On: Wed, 03 Jun 2015 15:54:11

band and Ge 3p XPS spectra taken at three different sputtering times referring to bulk Tm_2O_3 (Figs. 1(a) and 1(b)), interface (Figs. 1(c) and 1(d)) and Ge substrate (Figs. 1(e) and 1(f)). Since for Ge 3d, a strong presence of neighboring O 2s and Tm 5p doublet complicates the interpretation of the spectra,[16] in this work, Ge $3p_{3/2}$ and the centroid value of Tm 4d core-levels were used for VBO estimation. Figure 2(a) shows the peak areas of two components of O 1s core-level: from the main Tm_2O_3 (circle symbol) and from IL (triangle symbol). Each symbol point on the graphs refers to a single sputtering time, when the spectrum was taken. At first, the signal is dominated by the thulium contribution (until ~1100 s); however, as the sputtering through the film continues, the IL becomes more prominent until only interfacial layer species are left (at ~2000 s). These changes are further reflected in the plot of the Auger parameter, also shown in Fig. 2(a). The Auger parameter was calculated using the centroid values of the O 1s peak and from the O KLL Auger peak.[34] Note that in interfacial Tm_2O_3/Ge heterostructures, the Tm 4d core-levels exhibit a monotonically decreasing shift towards lower BEs of ~0.12 eV when sputtering Tm_2O_3 film (Figs. 1(c) and 2(b)), thus providing clear fingerprints of charging phenomenon.[25,26] On the contrary, a very small variation (~0.05 eV) of the Ge 3p BEs was observed (Figs. 1(d) and 2(c)). To account for the effect of differential charging, the positions of Tm 4d and Ge 3p peaks were estimated by extrapolating the measured BEs to zero Tm_2O_3 thickness (i.e., to the highest value of sputtering time in our experiment, see Fig. 2(a)), and hence ideally to zero charge.[25] The difference of Tm 4d and O 1s peaks was found to be 354.29 ± 0.03 eV, being indicative of the same stoichiometry of the films sputtered <2000 s. The value Tm 4d – Ge $3p_{3/2} = \delta_{INT} = 54.89$ eV was extracted from the extrapolated values in Figs. 2(b) and 2(c). Comparing the Ge $3p_{3/2}$ peak of the Ge substrate and the same peak with Tm_2O_3 on top, an energy shift towards higher BEs of 0.06 eV is observed. This is a signature of a small downward band bending, which agrees with the presence of p-type Ge.[35] The result suggests negligible bending of Ge core-levels despite the charging of the Tm_2O_3 film during x-ray exposure; a converse scenario has been observed for HfO_2/n-Ge.[28] The BE differences between Tm 4d centroid and VBM for bulk Tm_2O_3 (δ_{OXIDE}), and Ge $3p_{3/2}$ and VBM for the Ge substrate (δ_{SUB}) measured from Figs. 1(a) and 1(b) and Figs. 1(e) and 1(f), respectively, are summarized in Table I. By inserting δ_{OXIDE}, δ_{INT}, δ_{SUB} values in Kraut's equation (1), the $VBO = \delta_{SUB} + \delta_{INT} - \delta_{OXIDE} = 3.05 \pm 0.2$ eV is calculated for Tm_2O_3/Ge. The result is in agreement with our

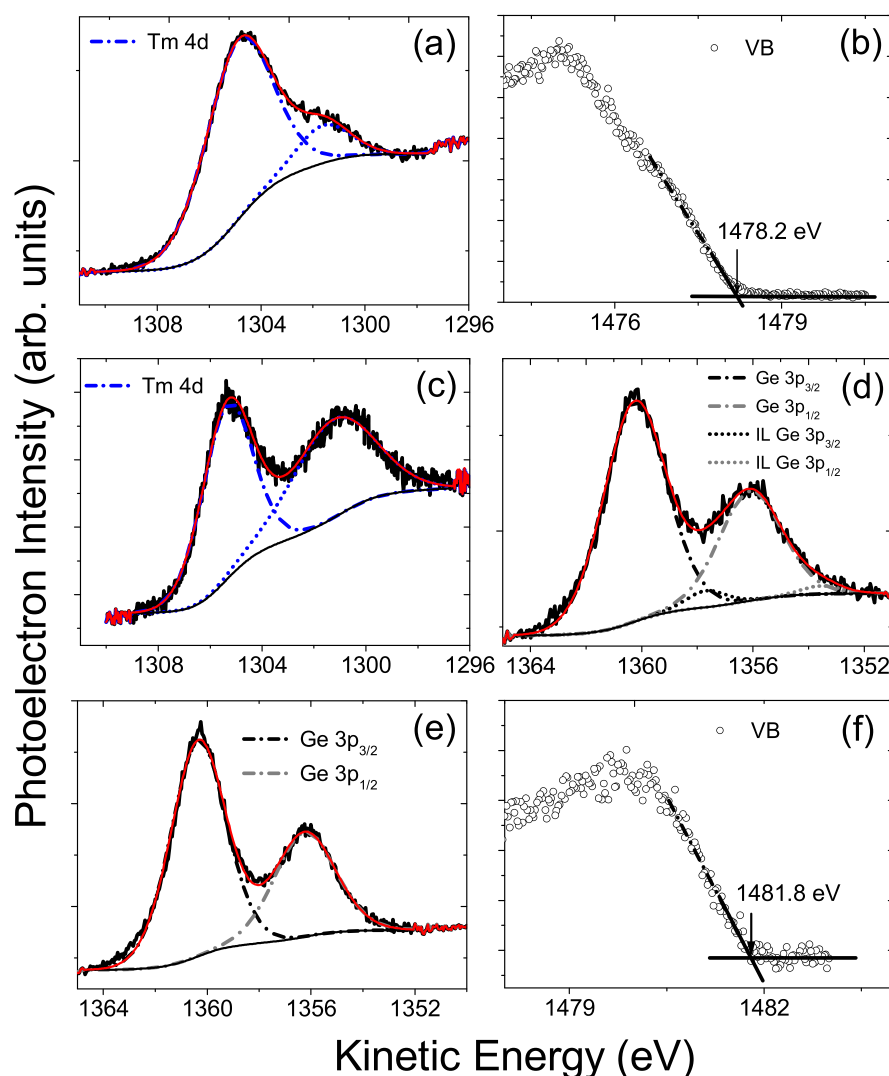

FIG. 1. Shallow core-levels and VB spectra for a bulk Tm_2O_3/Ge (a) and (b), an interfacial Tm_2O_3/Ge (c) and (d), and Ge substrate (e) and (f), recorded after sputtering for 210 s, 1470 s, and 2190 s, respectively. There is an additional peak (with spin-orbit splitting) for Ge 3p fitting in (d) due to IL contribution.

[This article is copyrighted as indicated in the article. Reuse of AIP content is subject to the terms at: http://scitation.aip.org/termsconditions. Downloaded to] IP: 138.253.76.166 On: Wed, 03 Jun 2015 15:54:11

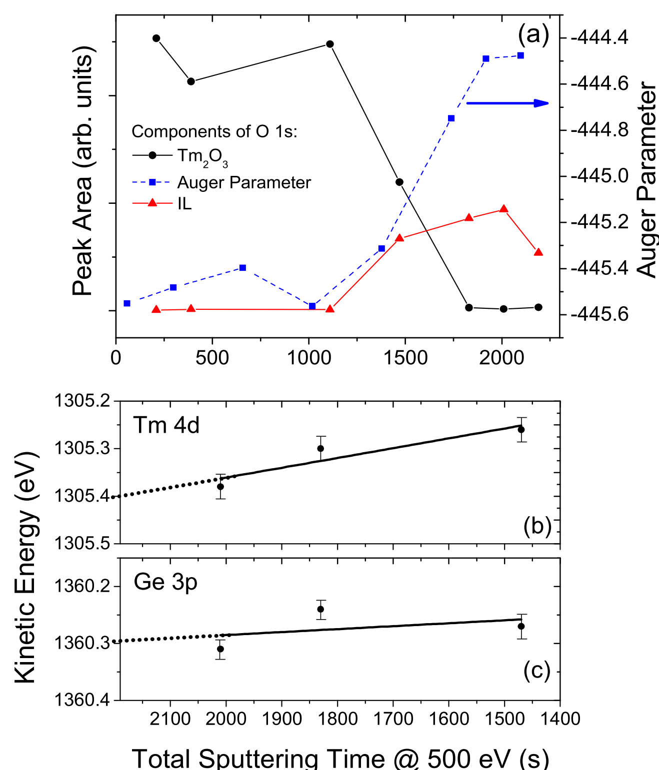

FIG. 2. (a) The peak area of the components of O 1s XPS core-level (left) and Auger parameter (right) as a function of total sputtering time. (b) and (c) The extrapolation of charge-corrected kinetic energies of Tm 4d and Ge $3p_{3/2}$ core-levels.

previously reported value of 2.95 ± 0.08 eV[16] from the XPS measurements taken on three distinctive samples.

B. Estimation of VBO for GeO_2/Ge gate stack

We now look to the estimation of VBO for the reference GeO_2/Ge system. Figs. 3(a) and 3(b) show high-resolution Ge 3d core-levels taken for bulk and interfacial GeO_2/Ge after prolonged (at least an hour) x-ray exposure, until the point they reached constant BEs.[17,25,26] The GeO_2 film shows two main peaks, fitted to doublets of Voigt functions with spin orbit splitting of 0.6 eV and branching ratio [1/2]. The difference between Ge $3d_{5/2}$ of the substrate (28.95 eV) and GeO_2 (32.34 eV) for the bulk sample is 3.4 eV, showing a stoichiometric GeO_2 and negligible differential charging.[17,36] Comparing the Ge $3d_{5/2}$ peak of the bare Ge (not shown) and the same peak from Ge with GeO_2 on top (Fig. 3(a)), an energy shift of 0.05 eV towards lower BEs is observed. The shift is consistent with n-Ge[20] and implies a 0.05 eV upward band bending at the GeO_2/n-Ge interface, in agreement with the formation of a superficial p-inversion layer in the n-type Ge substrates.[37] Note in Fig. 3(a) that the peak at ∼23 eV refers to O 2s CL, while three minor peaks in the energy range from 5 to 15 eV are part of VB and relate to O 2p, Ge 4s, and Ge 4p species in agreement with the literature.[20] The measured BE differences, δ_{OXIDE}, δ_{INT}, and δ_{SUB}, for GeO_2/Ge are listed in Table I and the literature values[17,20,28,38] are also inserted for comparison. Applying Kraut's equation (1), yields a $VBO = \delta_{SUB} + \delta_{INT} - \delta_{OXIDE} = 3.55 \pm 0.2$ eV, consistent with a value of 3.6 ± 0.2 eV reported by XPS[17] and by synchrotron radiation photoemission spectroscopy.[5]

C. Band gap evaluation and nature of Tm_2O_3/Ge interface

The band gaps of Tm_2O_3 and GeO_2 were determined by VUV-VASE. This was accomplished by first determining the thickness in the non-absorbing (transparent) region of the spectra. The dielectric function of the Ge film (31.9 nm) with the native oxide as Cauchy layer (1.4 nm) was modeled first. Then, another Cauchy layer is added and fitted for the thickness of Tm_2O_3 film (10.4 nm) or GeO_2 (4.6 nm). Subsequently, the optical constants (real and imaginary part of dielectric function) were extracted. The Tm_2O_3 (GeO_2) film was modelled with Cauchy layer at long wavelengths and extended into VUV with the B-spline and then converted to a general oscillator layer. The dielectric function converts to refractive index and extinction coefficient (k) using Kramers-Kronig relations. The absorption coefficient (α) is calculated from the extinction coefficient as $\alpha = 4\pi k/\lambda$, where λ is wavelength. The absorption coefficient vs photon energy plots for GeO_2/Ge and Tm_2O_3/Ge stacks are shown in Figs. 3(c) and 3(d), respectively. The band gap can be estimated by linear extrapolation of the segments on the curves in the non-absorbing regions, and is found to be 5.95 eV for GeO_2 and 5.77 eV for Tm_2O_3. The schematics of derived band line-ups for GeO_2/Ge and Tm_2O_3/Ge are depicted in Figs. 3(e) and 3(f). Note that both band gap values are slightly higher than those reported using the Tauc-Lorentz

TABLE I. Summary of XPS core-level energy differences measured for Tm_2O_3/Ge and GeO_2/Ge samples in this work and from the literature[17,20,28,38] with derived values of VBO and optical band gap.

	Tm_2O_3/p-Ge		GeO_2/n-Ge	
δ_{OXIDE} (eV)	Tm^{4d} – VBM	173.32	$Ge^{3d\ GeO2}$ – VBM	29.56 and 28.58[b]
δ_{INT} (eV)	Tm^{4d} – Ge^{3p}	54.89	$Ge^{3d\ GeO2}$ – $Ge^{3d\ sub}$	3.59 and 3.6[b]
δ_{SUB} (eV)	Ge^{3p} – VBM	121.48		
	Ge^{3d} – VBM	29.32, 29.30[a]	Ge^{3d} – VBM	29.52, 29.47,[b] 29.31,[c] and 29.36–29.58[d]
VBO (eV)	3.05		3.55	
Eg (α-method) (eV)	5.77		5.95	

[a]Ref. 17.
[b]Ref. 20.
[c]Ref. 28.
[d]Ref. 38.

[This article is copyrighted as indicated in the article. Reuse of AIP content is subject to the terms at: http://scitation.aip.org/termsconditions. Downloaded to] IP: 138.253.76.166 On: Wed, 03 Jun 2015 15:54:11

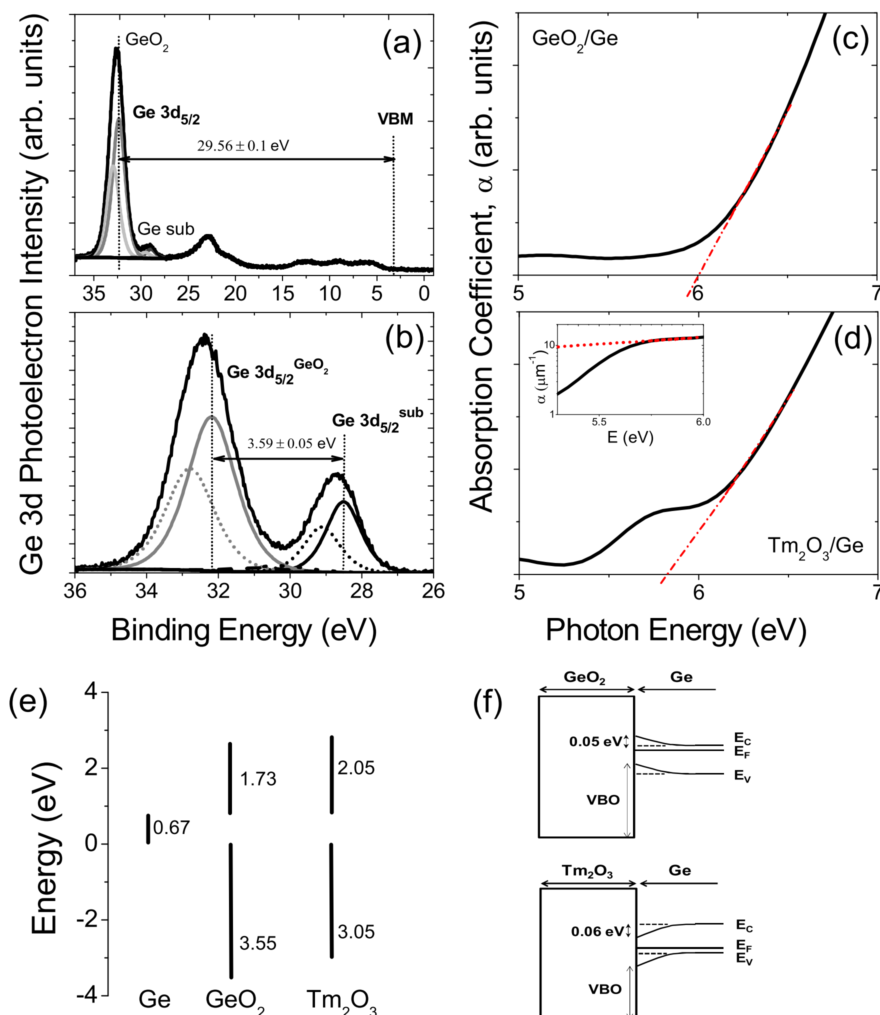

FIG. 3. The experimental and fitted Ge 3d XPS core-levels for (a) a thick 10 nm GeO_2/Ge, and (b) a thin 5 nm GeO_2/Ge. VBM refers to valence band maximum. Absorption coefficient vs photon energy extracted from VUV-VASE data for: (c) GeO_2/Ge and (d) Tm_2O_3/Ge. (e) The schematic of measured band gaps and hole barrier heights, where electron barrier heights, i.e., CBO is calculated using CBO = $E_{g(OXIDE)}$ − VBO − $E_{g(Ge)}$, where E_g refers to the band gap. (f) The schematic of experimentally observed band bending for GeO_2/n-Ge and Tm_2O_3/p-Ge in this work.

method,[16] in agreement with the finding of Di *et al.*[39] The band gap value for GeO_2 compares to Lange *et al.*,[40] where the optical band gap has been measured from an increase of the absorption edge and found to vary from 5.21 eV to 5.95 eV, depending on O_2 flow rate during reactive DC magnetron sputtering deposition. The band gap of 5.95 eV refers to highest O_2 flow and polycrystalline films of GeO_2. The band gap of GeO_2 of ∼6.0 eV has been reported from SE measurements from absorption edge.[41] The band gap value of Tm_2O_3 compares to 5.76 eV reported from optical reflectance on Tm_2O_3/Si stack.[13] It is worth noting a pronounced absorption (at ∼5.3 eV) below the band edge for the Tm_2O_3/Ge, and an Urbach tail (see inset of Fig. 3(d)) as a signature of the poly-crystalline nature[42] of the thulium oxide film.

The polycrystalline nature of the Tm_2O_3 deposited on Ge is directly seen from the HRTEM image and the electron diffraction pattern of Figs. 4(a) and 4(b) from which the cubic Tm_2O_3 structure has been identified. What is noticeable from the HRTEM image is the direct and sharp interface between the projected atomic structures of Ge and the Tm_2O_3 film (see white arrows in Fig. 4(b)), which is not the case for Tm_2O_3 deposited on Si, where a thin amorphous interfacial layer is observed (not shown). This feature is common to RE oxide or RE oxide-based films.[43–45] Some roughness is observed at this interface. From the chemical point of view, there is a transition region between the Ge

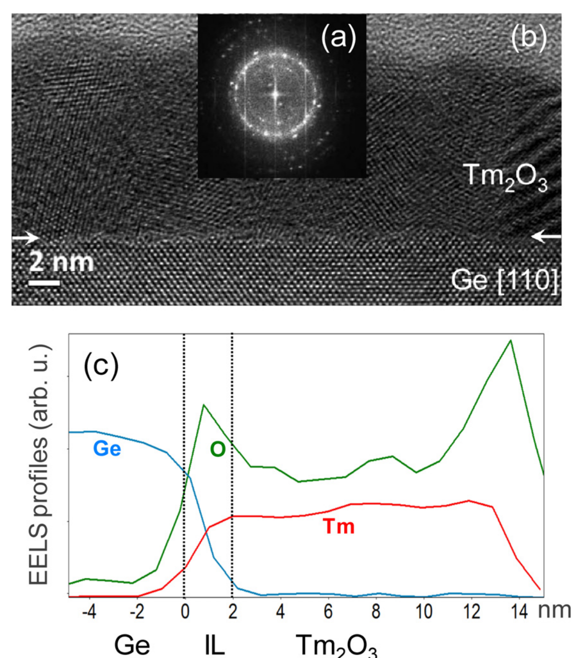

FIG. 4. Electron diffraction pattern (a), HRTEM image (b), and derived EELS elemental profiles across the interface (c), for 10 nm (nominal) Tm_2O_3 on Ge (white arrows in (b) help to locate the interface).

[This article is copyrighted as indicated in the article. Reuse of AIP content is subject to the terms at: http://scitation.aip.org/termsconditions. Downloaded to] IP: 138.253.76.166 On: Wed, 03 Jun 2015 15:54:11

substrate and the Tm_2O_3 film, where the three elements Tm, O, and Ge are present, as can be observed from calculated EELS elemental profiles in Fig. 4(c). Due to the 1 nm probe used for the EELS analysis, the transition region may point out to the roughness of this interface observed at the nanometer level and possibly to a chemically modified interface, at the sub-nanometer level, germanate in nature (Tm-O-Ge). The latter is further substantiated by the presence of a negligible IL peak ($<3\%$ area) from microscopic XPS measurements of Ge 3p CL shown in Fig. 1(d).

IV. SUMMARY

In summary, a consistent valence band offset value of $\sim$3 eV has been obtained for atomic-layer deposited Tm_2O_3/Ge from core-level and valence band XPS spectra measured at different sputtering times from a single bulk oxide layer. This method allows for more authentic probing of the interface, as there is no variation introduced when fabricating three separate samples for the XPS measurements. Furthermore, this study points unambiguously to both Tm_2O_3/Ge and GeO_2/Ge exhibiting sufficient conduction band offsets ($>$1.5 eV) to adequately suppress leakage current in real applications. The barrier role of Tm_2O_3 interlayer could suppress the growth of unstable GeO_x and bring effective passivation route in future Ge-based scaled CMOS devices.

ACKNOWLEDGMENTS

The work was funded by the EPSRC Grant No. EP/1012907/1, United Kingdom, and the European Research Grant 228229 OSIRIS. The VUV-VASE experiments were done at J.A. Woollam Co. Inc., NE, USA, courtesy of J. N. Hilfiker. The research leading to HRTEM/EELS results has received funding from the European Union Seventh Framework Programme under Grant Agreement No. 312483-ESTEEM2. M.A. acknowledges support from the Physics Department, Taif University, Saudi Arabia.

[1]K. Choi, T. Ando, E. Cartier, A. Kerber, V. Paruchuri, J. Iacoponi, and V. Narayanan, ECS Trans. **53**(3), 17 (2013).
[2]S. Takagi, R. Zhang, and M. Takenaka, Microelectron. Eng. **109**, 389 (2013).
[3]R. Zhang, W. Chern, X. Yu, M. Takenaka, J. L. Hoyt, and S. Takagi, Proc. IEEE IEDM Tech. Dig. **2013**, 633.
[4]K. Prabhakaran and T. Ogino, Surf. Sci. **325**, 263 (1995).
[5]M. Kobayashi, G. Thareja, M. Ishibashi, Y. Sun, P. Griffin, J. McVittie, P. Pianetta, K. Saraswat, and Y. Nishi, J. Appl. Phys. **106**, 104117 (2009).
[6]C. H. Lee, C. Lu, T. Tabata, W. F. Zhang, T. Nishimura, K. Nagashio, and A. Toriumi, Proc. IEEE IEDM Tech. Dig. **2013**, 40.
[7]S. Sioncke, H. C. Lin, A. Delabie, T. Conard, H. Struyf, S. De Gendt, and M. Caymax, ECS J. Solid State Sci. Technol. **1**(3), P127 (2012).
[8]M. Kouda, T. Kawanago, P. Ahmet, K. Natori, T. Hattori, H. Iwai, K. Kakushima, A. Nishiyama, N. Sugii, and K. Tsutsui, J. Vac. Sci. Technol. B **29**(6), 062202 (2011).
[9]M. Kouda, K. Kakushima, P. Ahmet, K. Tsutsui, A. Nishiyama, N. Sugii, K. Natori, T. Hattori, and H. Iwai, Jpn. J. Appl. Phys. **50**(10), 10PA04 (2011).
[10]T. Ji, J. Cui, Z. B. Fang, T. X. Nie, Y. L. Fan, X. L. Li, Q. He, and Z. M. Jiang, J. Cryst. Growth **321**, 171 (2011).
[11]H. Iwai, S. Ohmi, S. Akama, C. Ohshima, A. Kikuchi, I. Kashiwagi, J. Taguchi, H. Yamamoto, J. Tonotani, Y. Kim, I. Ueda, A. Kuriyama, and Y. Yoshihara, Proc. IEEE Int. Electron Devices Meet. **2002**, 625.
[12]J. J. Wang, Z. B. Fang, T. Ji, W. Y. Ren, Y. Y. Zhu, and G. He, Appl. Surf. Sci. **258**, 6107 (2012).
[13]J. Wang, T. Ji, Y. Zhu, Z. Fang, and W. Ren, J. Rare Earth **30**, 233 (2012).
[14]E. Dentoni Litta, P.-E. Hellstrom, C. Henkel, S. Valerio, A. Hallen, and M. Ostling, J. Electrochem. Soc. **160**(11), D538 (2013).
[15]E. Dentoni Litta, P-E. Hellström, C. Henkel, and M. Östling, IEEE Trans. Electron Devices **60**(10), 3271 (2013).
[16]I. Z. Mitrovic, M. Althobaiti, A. D. Weerakkody, N. Sedghi, S. Hall, V. R. Dhanak, P. R. Chalker, C. Henkel, E. Dentoni Litta, P.-E. Hellström, and M. Östling, Microelectron. Eng. **109**, 204 (2013).
[17]W. F. Zhang, T. Nishimula, K. Nagashio, K. Kita, and A. Toriumi, Appl. Phys. Lett. **102**, 102106 (2013).
[18]L. Lin, K. Xiong, and J. Robertson, Appl. Phys. Lett. **97**, 242902 (2010).
[19]M. Yang, R. Q. Wu, Q. Chen, W. S. Deng, Y. P. Feng, J. W. Chai, J. S. Pan, and S. J. Wang, Appl. Phys. Lett. **94**, 142903 (2009).
[20]M. Perego, G. Scarel, M. Fanciulli, I. L. Fedushkin, and A. A. Skatova, Appl. Phys. Lett. **90**, 162115 (2007).
[21]Y. Fukuda, Y. Yazaki, Y. Otani, T. Sato, H. Toyota, and T. Ono, IEEE Trans. Electron Devices **57**(1), 282–7 (2010).
[22]P. Broqvist, J. F. Binder, and A. Pasquarello, Appl. Phys. Lett. **98**, 129901 (2011); P. Broqvist, J. F. Binder, and A. Pasquarello, Appl. Phys. Lett. **94**, 141911 (2009).
[23]P. Broqvist, J. F. Binder, and A. Pasquarello, Microelectron. Eng. **88**, 1467–1470 (2011).
[24]R. Puthenkovilakam and J. P. Chang, J. Appl. Phys. **96**, 2701 (2004).
[25]M. Perego and G. Seguini, J. Appl. Phys. **110**, 053711 (2011).
[26]E. Bersch, M. Di, S. Consiglio, R. D. Clark, G. J. Leusink, and A. C. Diebold, J. Appl. Phys. **107**, 043702 (2010).
[27]O. Engstrom, J. Appl. Phys. **112**, 064115 (2012).
[28]M. Perego, A. Molle, and G. Seguini, Appl. Phys. Lett. **101**, 211606 (2012).
[29]E. Kraut, R. Grant, J. Waldrop, and S. Kowalczyk, Phys. Rev. Lett. **44**, 1620 (1980).
[30]S. A. Chambers, T. Droubay, T. C. Kaspar, and M. Gutowski, J. Vac. Sci. Technol. B **22**, 2205 (2004).
[31]M. T. Anthony, in *Spectrometer Calibration; Practical Surface Analysis by Auger and X-ray Photoelectron Spectroscopy*, edited by D. Briggs and M. P. Seah (Wiley, New York, 1988), p. 429.
[32]J. C. Vickerman, *Surface Analysis* (John Wiley, 1998).
[33]D. A. Shirley, Phys. Rev. B **5**, 4709 (1972).
[34]R. J. Cole, D. A. C. Gregory, and P. Weightman, Phys. Rev. B **49**(8), 5657 (1994).
[35]J. S. Hovis, R. J. Hamers, and C. M. Greenlief, Surf. Sci. **440**, L815 (1999).
[36]T. Sasada, Y. Nakakita, M. Takenaka, and S. Takagi, J. Appl. Phys. **106**, 073716 (2009).
[37]A. Dimoulas, P. Tsipas, A. Sotiropoulos, and E. K. Evangelou, Appl. Phys. Lett. **89**, 252110 (2006).
[38]M. K. Hudait, Y. Zhu, D. Maurya, S. Priya, P. K. Patra, A. W. K. Ma, A. Aphale, and I. Macwan, J. Appl. Phys. **113**, 134311 (2013).
[39]M. Di, E. Bersch, A. C. Diebold, S. Consiglio, R. D. Clark, G. J. Leusink, and T. Kaack, J. Vac. Sci. Technol. A **29**(4), 041001 (2011).
[40]T. Lange, W. Njoroge, H. Weis, M. Beckers, and M. Wuttig, Thin Solid Films **365**, 82 (2000).
[41]C. H. Lee, T. Tabata, T. Nishimura, K. Nagashio, K. Kita, and A. Toriumi, ECS Trans. **19**, 165 (2009).
[42]F. L. Martinez, M. Toledano-Luque, J. J. Gandia, J. Carabe, W. Bohne, J. Rohrich, E. Strub, and I. Martil, J. Phys. D: Appl. Phys. **40**, 5256 (2007).
[43]L. Lamagna, C. Wiemer, M. Perego, S. N. Volkos, S. Baldovino, D. Tsoutsou, S. Schamm-Chardon, P. E. Coulon, and M. Fanciulli, J. Appl. Phys. **108**, 084108 (2010).
[44]S. Schamm-Chardon, P. E. Coulon, L. Lamagna, C. Wiemer, S. Baldovino, and M. Fanciulli, Microelectron. Eng. **88**, 419 (2011).
[45]S. Schamm-Chardon, in *Transmission Electron Microscopy in Micro-Nanoelectronics*, edited by A. Claverie and M. Mouis (John Wiley and Sons, New York, 2013), p. 135.

[This article is copyrighted as indicated in the article. Reuse of AIP content is subject to the terms at: http://scitation.aip.org/termsconditions. Downloaded to] IP: 138.253.76.166 On: Wed, 03 Jun 2015 15:54:11